(12) INTERNATIONAL APPLICATION PUBLISHED UNDER THE PATENT COOPERATION TREATY (PCT)

(19) World Intellectual Property Organization
International Bureau

(43) International Publication Date
26 June 2025 (26.06.2025)

WIPO | PCT

(10) International Publication Number
WO 2025/129339 A1

(51) International Patent Classification:
G01N 27/12 (2006.01)

(21) International Application Number:
PCT/CA2024/051696

(22) International Filing Date:
19 December 2024 (19.12.2024)

(25) Filing Language: English

(26) Publication Language: English

(30) Priority Data:
63/611,945 19 December 2023 (19.12.2023) US

(71) Applicant: **MCMASTER UNIVERSITY** [CA/CA]; 1280 Main Street West, Hamilton, Ontario L8S 4L8 (CA).

(72) Inventors: **KRUSE, Peter**; 33 Norwood Road, Hamilton, Ontario L8S 3P8 (CA). **DARESTANIFARAHANI, Maryam**; 4140 Foxwood Drive, Burlington, Ontario L7M 4R4 (CA). **SELVAGANAPATHY, Ponnambalam Ravi**; 10 Griffin Road, Dundas, Ontario L9H 6S2 (CA).

(74) Agent: **SMART & BIGGAR LP**; 40 King Street West, 40th Floor, Toronto, Ontario M5H 3Y2 (CA).

(81) Designated States *(unless otherwise indicated, for every kind of national protection available)*: AE, AG, AL, AM, AO, AT, AU, AZ, BA, BB, BG, BH, BN, BR, BW, BY, BZ, CA, CH, CL, CN, CO, CR, CU, CV, CZ, DE, DJ, DK, DM, DO, DZ, EC, EE, EG, ES, FI, GB, GD, GE, GH, GM, GT, HN, HR, HU, ID, IL, IN, IQ, IR, IS, IT, JM, JO, JP, KE, KG, KH, KN, KP, KR, KW, KZ, LA, LC, LK, LR, LS, LU, LY, MA, MD, MG, MK, MN, MU, MW, MX, MY, MZ, NA, NG, NI, NO, NZ, OM, PA, PE, PG, PH, PL, PT, QA, RO, RS, RU, RW, SA, SC, SD, SE, SG, SK, SL, ST, SV, SY, TH, TJ, TM, TN, TR, TT, TZ, UA, UG, US, UZ, VC, VN, WS, ZA, ZM, ZW.

(54) Title: ION SELECTIVE SENSOR

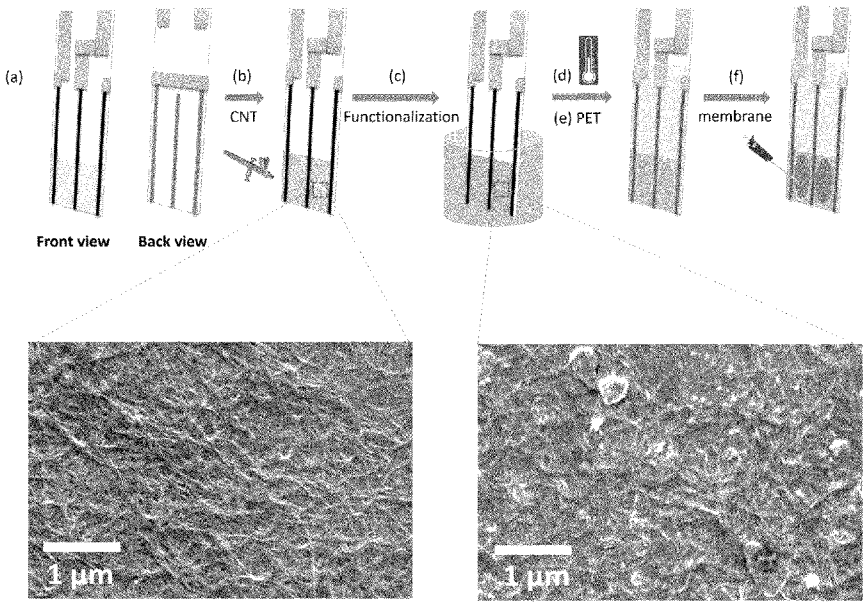

FIG. 1

(57) Abstract: The present disclosure relates to solid-state sensors that exploit a unique sensing mechanism which amplifies the response of ion-selective membranes (ISM) several fold. In the presence of the analyte, such as lead, the binding sites within the membrane bind with the analyte modulating the interactions between the binding sites and the chemiresi stive film. This competitive binding provides a higher sensitivity when compared with conventional ion-selective electrode configurations. It also differs from a simple chemiresistor covered with an ISM because the reference electrode can be eliminated. The impact of these interactions on the conductivity of the film can also be maximized by its surface treatment, ultimately achieving a lower level of detection than possible with potentiometric methods. Sensors developed using this design may be employed as aqueous continuous in situ ion sensors to detect harmful levels of analytes in surface, drinking, or wastewater.

WO 2025/129339 A1

[Continued on next page]

(84) Designated States *(unless otherwise indicated, for every kind of regional protection available)*: ARIPO (BW, CV, GH, GM, KE, LR, LS, MW, MZ, NA, RW, SC, SD, SL, ST, SZ, TZ, UG, ZM, ZW), Eurasian (AM, AZ, BY, KG, KZ, RU, TJ, TM), European (AL, AT, BE, BG, CH, CY, CZ, DE, DK, EE, ES, FI, FR, GB, GR, HR, HU, IE, IS, IT, LT, LU, LV, MC, ME, MK, MT, NL, NO, PL, PT, RO, RS, SE, SI, SK, SM, TR), OAPI (BF, BJ, CF, CG, CI, CM, GA, GN, GQ, GW, KM, ML, MR, NE, SN, TD, TG).

Declarations under Rule 4.17:

— *as to applicant's entitlement to apply for and be granted a patent (Rule 4.17(ii))*

Published:

— *with international search report (Art. 21(3))*

— *in black and white; the international application as filed contained color or greyscale and is available for download from PATENTSCOPE*

ION SELECTIVE SENSOR

CROSS-REFERENCE TO RELATED APPLICATION

This application claims priority to U.S. Provisional Application No. 63/611,945 filed on December 19, 2023, the entire contents of which are hereby incorporated herein by reference.

FIELD

The present disclosure relates to the development of solid-state sensors. The sensor design exploits a unique sensing mechanism that can amplify the response of ion-selective membranes (ISM) several fold. A semi-conductive or conductive film comprised of carbon nanotubes (CNT) may be coated with a suitable ligand to create a chemiresistor. The chemiresistive film is then coated with an ion-selective membrane embedded with ionophores. The chemiresistive film and the analyte of interest competitively bind to the ionophores in the ISM. In the presence of the analyte, the binding sites within the membrane bind with the analyte modulating the interactions between the binding sites and the chemiresistive film. This competitive binding provides a higher sensitivity when compared with conventional ion-selective electrode configurations wherein the electrode serves only as an electrical conductor to transduce the changes in potential of the ISM. It also differs from a simple chemiresistor covered with the ISM because the reference electrode can be eliminated but the response was still due to polarization caused by the accumulation of ions in the ion-selective layer. The impact of these interactions on the conductivity of the film is maximized by its surface treatment, ultimately achieving a lower level of detection (LoD) than possible with potentiometric methods (in addition to eliminating the need for a reference electrode). Such sensors may be used as aqueous ion sensors to detect harmful levels of analytes in surface, drinking, or wastewater. Chemiresistive sensors developed by this method employ a specific mechanism that can achieve lower detection limits than potentiometric devices while being more robust and easier to fabricate by omitting the reference electrode. The proposed technology and resulting mechanism may also be applied to ChemFETs in their various geometries (backgated or solution gated, extended gate, etc.). One implementation of the proposed technology is the development of a highly sensitive ion-selective chemiresistive sensor for *in situ* continuous monitoring of lead ions (Pb^{2+}) in water.

BACKGROUND

The following paragraphs are not an admission that anything discussed in them is prior art or part of the knowledge of the person of ordinary skill in the art.

Lead continuous to be one of the most dangerous drinking water contaminants and its presence in residential areas is frequently attributed to outdated building infrastructure containing lead pipes. According to the World Health Organization (WHO), the maximum acceptable concentration (MAC) of lead in drinking water is 10 µg/L. Exposure can come from corrosion of plumbing materials, or obtaining water from contaminated sources, as seen in Flint, Michigan. Currently, monitoring of lead is commonly done by random daytime sampling (RDT) which requires sample collection, treatment and inductively coupled plasma-mass spectrometry (ICP-MS), inductively coupled plasma-atomic emission spectrometry (ICP-AES), atomic adsorption spectroscopy (AAS), fluorescence or Anodic stripping voltammetry (ASV). These laboratory analysis techniques are time-consuming, not easily accessible, and costly due to the instrumentation used.

Methods currently under development are optical, electrochemical and electrical sensors which are aiming to be used for in-situ detection of Pb^{2+} in drinking water in addition to meeting the standards for a sensor such as highly accurate, precise and sensitive response. For instance, a type of colorimetric test strips has been commercialized by MQuant which semi-quantitatively measures Pb^{2+} concentration from 20 to 500 mg/L based on the complex formation between Rhodizonic acid and lead in acidic solutions. To accurately quantify lower concentrations of lead, a photometric reagent lead test kit made by Spectroquant is available on market. It can measure Pb^{2+} ions in a range of 10 µg/L to 5 mg/L by complex formation of Pb^{2+} ions with 4-(2'-pyridylazo)resorcinol (PAR) in alkaline solutions. Two ion-selective electrodes (ISEs) have been commercialized by Thermo Scientific (measuring 10^{-6} M to 0.1 M (0.2 mg/L to 20,700 mg/L) of Pb^{2+} in a pH range of 4-7)[12] and Mettler Toledo (measuring 10^{-5} M to 1.0 M (2 mg/L to 207,000 mg/L) of Pb^{2+} in pH 2 to 8)[13] using ion-selective membrane (ISM) technology. Although these sensors allow for fast and easy measurement of Pb^{2+} ions in-situ, they still lack sufficient sensitivity.

Moreover, several advanced optical and electrical Pb^{2+} sensors have been reported which have high sensitivity. For instance, a rapid analytical ion-sensing platform using smart hydrogels and working based on the dye release from hydrogels entrapping ion-selective microdroplets was introduced by Du et al. which was able to measure the Pb^{2+} concentration with a detection limit of 62 µg/L. Ghosh et al. prepared an optical fiber grating functionalized with glutaraldehyde cross-linked chitosan (CCS), nitrogen-doped graphene oxide (NGO) nanocomposites, and poly(acrylic acid) (PAA). The sensor surface was modified by hydroxylation and self-assembly of CCS-NGO/PAA layers, resulting in a detection limit of 0.10 µg/L. One of the main problems of optical devices is that they require reagents to react with the analyte. A number of electrochemical sensors for Pb^{2+} ions have also been reported, for example as developed by the Molinero-Abad group with a detection limit of 0.07 µg/L. Anodic stripping voltametric method was used as a method of detection, with the surface of the working electrode modified by single-walled carbon nanotubes, electro-reduced graphene oxide and electrogenerated gold nanoparticle. Yu et al. modified a Pb^{2+}-selective electrode using a conducting polymer-poly(2-methoxy-5-(2'-ethylhexyloxy)-p-phenylene vinylene) (MEH-PPV) as an ion-to-electron transducer which resulted in a detection limit of 0.13 µg/L. However, electrochemical sensors such as potentiometric ion-selective electrodes (ISE) require reference electrodes, increasing fabrication costs, and causing stability issues.

Sensors based on field-effect transistor (FET) geometries can improve sensitivity at the expense of increased complexity. Zhou et al. developed a real-time and selective Pb^{2+} sensor in a FET geometry with a reduced graphene oxide (rGO) film as a semiconducting channel modified with gold nanoparticles and L-glutathione. It responded sensitively and selectively to Pb^{2+} ions in a concentration range of 10 nM to 10 µM with 11% response at 10 µM in 1 to 2 seconds. The proposed sensing mechanism was that holes of the p-doped channel are forced away from the gate insulator-semiconductor interface by the positive electrical field formed by Pb^{2+} ions. Thus, a depletion layer is created, resulting in a drop in current. Despite the high sensitivity of these solid-state devices, there are several interferants in real samples that affect their response. In addition, their complicated geometry increases their cost.

Chemiresistive sensors are solid state devices with a similar working principle to FET sensors, but a simpler design since they operate without a gate (i.e. at zero gate voltage). They

work by detecting electrical current changes across the resistive film caused by its interaction with the target analyte. These sensors do not require reagents, reference electrodes, or expensive instrumentation. However, they have not yet been successfully employed for lead detection. A reported chemiresistor with a resistive film made from β-cyclodextrin (BCD) functionalized reduced graphene oxide (rGO) has an unacceptably high limit of detection (LoD) of 10 mg/L. Selectivity has also been a challenge in the development of chemiresistive devices. Recently, a new ion-selective chemiresistive platform was introduced by the inventors of the present disclosure for detecting nitrate, nitrite and ammonium. A top layer of ion-selective membrane (ISM) simultaneously protects the sensors surfaces and enhances their selectivity. In order to be relevant for Pb^{2+} detection, the sensitivity of the platform needs to be enhanced further.

The use of carbon nanotubes and ion selective membranes embedded with ionophores as sensors has been disclosed in patent documents, namely US10900925B2, US20230003684A1, CN113588754B and TWI517989B. Some journal publications have studied applying CNT to improve the sensitivity and selectivity of ISMs. However, functionalizing single-walled carbon nanotubes (SWCNTs) with ligands and using them in conjunction with ionophores in the ISM to create the unique binding mechanism has not been previously considered as a method to develop highly sensitive ion-selective chemiresistive sensors.

INTRODUCTION

The following is intended to introduce the reader to the detailed description that follows and not to define or limit the claimed subject matter.

The present disclosure demonstrates an ion-selective chemiresistive sensor capable of continuously monitoring concentrations of Pb^{2+} in water well below regulatory thresholds. To achieve the objective, two strategies were employed. Firstly, by modifying the resistive film with a solution of NaOH and 15-crown-5 ether to tune the electrical properties of the film and, and secondly by improving the sensor fabrication process. The device consists of a conducting CNT film coated with a Pb^{2+}-selective membrane. The thicknesses of the conducting film (resistive film) and the membrane were optimized. Sensitivity, selectivity, stability, and reversibility of the sensors are investigated, and the sensing mechanism is discussed. Improvements to the sensitivity and

stability of the devices for detection of heavy metals make them suitable for *in situ* analysis, increasing the accessibility of lead testing for the general public.

BRIEF DESCRIPTION OF THE DRAWINGS

The drawings included herewith are for illustrating various examples of apparatuses and methods of the present disclosure and are not intended to limit the scope of what is taught in any way.

Figure 1 shows a sensor fabrication process. (a) Front and back views of three screen-printed contacts and copper tape connections, (b) air brushing CNT on the frosted part of the glass slide and SEM image of the resulting CNT film, (c) functionalizing the CNT film with 0.1 M of NaOH.15-crown-5 ether solution and SEM image of the resulting n-doped CNT film, (d) curing the sensor at 85 °C, (e) applying pre-cut clear PET sheet to cover the contacts and have specific openings, (f) drop-casting ISM solution into the openings and drying for 12 hours.

Figure 2 shows lead (II) sensor modification by functionalization of the resistive film and improving the sensor fabrication. (a) Signal-to-noise ratio (blue bars) and %RSD (orange bars) values of various lead (II) sensors: 1. made of air-brushed SWCNT film coated with ISM and two copper contacts, 2. made of air-brushed f-SWCNT film coated with ISM and three screen-printed (SP) carbon contacts , (b) Image of an actual lead (II) sensor with two copper contacts geometry, (c) Image of an actual lead (II) sensor with three screen-printed (SP) carbon contacts geometry.

Figure 3 shows (a) structure of lead ionophore IV, tert-Butylcalix[4]arene-tetrakis(N,N-dimethylthioacetamide), (b) percent sensor response of bare (resistive film: f-SWCNT), blank (resistive film: f-SWCNT coated with blank membrane without ionophore) and Pb^{2+} sensors (resistive film: f-SWCNT coated with ISM) to 10 µg/L (blue bars), 33 µg/L (orange bars) and 100 µg/L (gray bars) of Pb^{2+} in 200 mg/L tris-acetate buffer solution at pH 5.5.

Figure 4 shows (a) Pb^{2+}-selective chemiresistive sensor response to Pb^{2+} over time in 200 mg/L tris-acetate buffer solution at pH 5.5, (b) calibration curve of the sensor response vs. the concentration of Pb^{2+} (in a concentration range of 3.3-3300 µg/L) fitted with a Langmuir equation (fitting parameters, A and B are 7.53% and 0.0048 L/µg respectively), inset: calibration curve of the sensor in the lower range only (3.3-100 µg/L) with fitting parameters, A and B, 2.96% and

0.049 L/µg respectively, (c) linearized calibration curve of the fabricated sensor vs. the concentration of Pb^{2+} (in a concentration range of 3.3-3300 µg/L), inset: zoomed-in linearized calibration curve of the sensor in lower concentrations (3.3-100 µg/L), (d) average response time as a function of Pb^{2+} concentration in a range of 3.3-3300 µg/L.

Figure 5 shows selectivity test of the fabricated Pb^{2+} sensor in 200 mg/L tris-acetate buffer solution at pH 5.5. Response of the Pb^{2+} sensor to 10 µg/L Pb^{2+} in the presence of interfering ions at common concentrations in drinking water.

Figure 6 shows Hall coefficients and Hall mobilities after each fabrication step, Pb^{2+} exposure and recovery, accompanied by a schematic of the resistive film at each step. Inset: image of the fabricated four-probe device for Hall measurements.

Figure 7 shows sensing mechanism of a Pb^{2+} ion-selective chemiresistive sensor. (a) cross-sectional view of the slightly n-doped f-SWCNT resistive film, (b) coated with ISM which turned it p-doped and (c) immersed in the background solution and exposed to Pb^{2+} ions which decreased the number of holes.

Figure 8 shows sensitivity comparison of a bare device and a Pb^{2+} sensor to lead ions in different concentrations (from 33 ppb to 3.3 ppm). (a) Response of a bare sensor made of SWCNT as a resistive film and (b) a Pb^{2+} sensor made of SWCNT as a resistive film and coated with ISM (drop-casted 50 µL of ISM solution on the SWCNT at the circular opening (image of the actual sensor on the top right of the figure).

Figure 9 shows a response comparison of a Pb^{2+} sensor and a bare sensor to lead ions in different concentrations (from 1 ppb to 3.3 ppm). (a) Response of a Pb^{2+} sensor made of f-SWCNT (with NaOH.15-crown-5 ether) as a resistive film coated with ISM (drop-casted 50 µL of ISM solution on the SWCNT film at the circular opening) and (b) a bare sensor made of f-SWCNT (with NaOH.15-crown-5 ether) as a resistive film (image of the actual sensor on the top right of the figure).

Figure 10 shows Pb^{2+} sensor responses in a range of pH 4-7 in 200 mg/L tris-acetate buffer solution.

Figure 11 shows sensor response (current changes) of a fabricated Pb2+ sensor to various concentrations between 1 ppb to 3.3 ppm vs. time over three cycles. (a) Sensor response in first cycle, (b) sensor response in second cycle, (c) sensor response in third cycle.

Figure 12 shows SEM images of air-brushed CNT films of three different batches in two bar scales of 100 µm and 10 µm. (a & b) SEM images of a representative CNT film of batch No. 1 (resistance 9.2 kΩ), (c & d) batch No. 2 (resistance 5.5 kΩ), (e & f) batch No. 3 (resistance 12.3 kΩ).

Figure 13 shows responses of several fabricated Pb^{2+} sensors and their recovery over time in a Pb^{2+} concentration range of 1 ppb to 3.3 ppm. (a) Performance of Pb^{2+} sensor#2, (b) Pb^{2+} sensor#3, (c) Pb^{2+} sensor#4, and (d) Pb^{2+} sensor#5.

Figure 14 shows (a) lead sensor's response and recovery between 0 ppb and 3300 ppb of Pb^{2+} ions, (b) absolute values of response and recovery percentages of a fabricated lead sensor between 0 ppb and 3300 ppb of Pb^{2+} ions over three cycles.

Figure 15 shows calibration curves of Pb^{2+} sensors prepared for real sample test and the response of the sensor to 10 ppb and 30 ppb of Pb^{2+} ion. (a) Calibration curve of sensor#1, (b) sensor#2 and (c) sensor#3 in tap water in a range of 10 ppb to 330 ppb of Pb^{2+} ions, (d) response of the sensor#1 to 10 ppb of Pb^{2+}, (e) response of the sensor#2 to 10 ppb of Pb^{2+}, and (f) response of the sensor#3 to 33 ppb of Pb^{2+} over three cycles (n=3) in tap water.

Figure 16 shows Raman spectra of pristine CNT, n-doped CNT and n-doped CNT exposed to 3 ppm of Pb^{2+} ions for 5 hours.

DETAILED DESCRIPTION

Various apparatuses or methods will be described below to provide an example of an embodiment of each claimed invention. No embodiment described below limits any claimed invention and any claimed invention may cover apparatuses and methods that differ from those described below. The claimed inventions are not limited to apparatuses and methods having all of the features of any one apparatus or method described below, or to features common to multiple or all of the apparatuses or methods described below. It is possible that an apparatus or method described below is not an embodiment of any claimed invention. Any invention disclosed in an

apparatus or method described below that is not claimed in this document may be the subject matter of another protective instrument, for example, a continuing patent application, and the applicant(s), inventor(s) and/or owner(s) do not intend to abandon, disclaim or dedicate to the public any such invention by its disclosure in this document.

Experimental methods

Materials, reagents and apparatus

Lead (II) nitrate, tris(hydroxymethyl)aminomethane, 99.7% glacial acetic acid (ACS reagent grade), single walled carbon nanotubes (6.5 chirality, ≥95% carbon nanotubes, 0.78 nm average diameter), 15-crown-5 ether, poly vinyl chloride (PVC), 2-nitrophenyl octyl ether (o-NPOE), lead ionophore IV (tert-nutylcalix[4]arene-tetrakis(N,N-dimethylthioacetamide), potassium tetrakis[3,5-bis(trifluoromethyl)phenyl]borate (KTFBP), methanol (anhydrous), acetone (ACS reagent), tetrahydrofuran (THF) were purchased from Sigma-Aldrich. Sodium hydroxide Certified A.C.S Pellets (P250-500) were purchased from Fisher Chemicals. Ultrapure water (18.2 MΩ·cm) was obtained from a Millipore Simplicity 185 purification system. Acetic acid was prepared by diluting glacial acetic acid into ultrapure water.

Twin frosted glass slides (75×25×1 mm^3) were purchased from VWR, Carbon ink 124-39 (EU) was produced by Creative Materials Inc., ¼" wide adhesive copper tape (3M #1181) purchased from 3M. Roller, thread sealing tape (PTFE) - 1⁄2 × 520" and transparent adhesive Polyethylene terephthalate (PET) sheet (thickness 60 ± 8 µm) were purchased from Uline. A Cricut (Provo Craft & Novelty Inc.) low-cost cutting plotter was used to pattern the mask and the PET sheet. A gravity-fed air-brush gun (NEO for Iwata, 0.35 mm nozzle) was used with an air compressor. During the experiment, current changes were measured using EPU 452 Quad MF isoPod four channel electronics from eDAQ Pty Ltd.

For surface characterizations, SEM images were taken with JEOL 7000 Analytical SEM of airbrushed SWCNTs and f-SWCNTs on silicon/silicon dioxide (thermally grown) chips (1×1 cm^2) with resistances similar to the sensor with an acceleration voltage of 3 kV and 10.000X magnification. Hall measurements were performed with a Nanometric HL 5500PC Hall effect measurement system on Si/SiO_2 chips (1×1 cm^2) as well with four sputter coated Cr-Au contacts in van der Pauw geometry. CNTs were air brushed inside a contact mask at the center of the device

with a target resistance of 9 or 10 kΩ. Raman spectra were obtained on a Renishaw inVia Raman spectrometer with a 633 nm laser. 1% laser power and a 20× objective lens were used to collect the spectra with a 12 s exposure time and two runs on different spots with 10 accumulations on each run. It was possible to characterize the surface at three different fabrication steps: first step, air-brushed pristine SWCNT film on the frosted part of the glass slide; second step, n-doped and protected f-SWCNT film with NaOH.15-crown-5 ether mixture; and third step: the prepared films were exposed to a solution containing 3 mg/L of Pb^{2+} for 5 hours. It was not feasible to characterize CNT films covered with membranes since the membranes are very thin and easily torn during removal.

Sensor fabrication

Prior to the fabrication process, 2 mg of SWCNT powder was dispersed in 15 ml of methanol in a bath sonicator (Elmasonic P30H Ultrasonic Cleaner) at 30°C, 37 kHz and 100% power for six hours. The ISM solution for Pb^{2+} ions was prepared from 5 mg of ionophore IV, 33 mg PVC, 65 mg 2-nitrophenyl-octyl ether (o-NPOE) and 1 mg KTFBP dissolved in 2 ml of THF.

Three conductive contacts are screen printed with carbon ink on the glass slide serving as a base for each sensor. The first and third contacts were connected with copper tape at the back. The chemiresistor was attached to the measurement electronics with one alligator clip connected to those contacts, and the other alligator clip attached to the middle contact (Fig. 1a). Afterwards, the frosted part of the glass slide was rinsed with methanol, and the edges of the frosted area were masked by Teflon tape. Then, the dispersed CNT solution was airbrushed onto the substrate at 50 °C until the resistance reached 9 kΩ (Fig. 1b) followed by removing the Teflon tape and immersing the sensors in a mixture of 0.1 M NaOH and 0.1 M 15-crown-5 ether solution in methanol at room temperature for an hour to make functionalized SWCNTs (f-SWCNTs) (Fig. 1c). After functionalization, the sensor was rinsed three times with methanol and cured in an oven at 85 °C for one hour (Fig. 1d). Subsequently, the contacts were covered with pre-cut clear adhesive PET sheet with two oval openings (7 mm × 1.8 mm) to isolate the contact regions from exposure to the sample (Fig. 1e). After that, 50 µL of prepared ion-selective membrane (ISM) solution were drop-cast into each opening and left to dry for 12 hours (Fig. 1f). Subsequently, sensors were immersed

in a 3 mg/L $Pb(NO_3)_2$ conditioning solution at pH 5.5 for 24 hours to activate the ionic sites to be able to exchange the Pb^{2+} easier and faster.

Sensor testing

For each experiment, a batch of four sensors (includes three Pb^{2+} sensors and one blank as a control) were fabricated and tested for 3 cycles. Following the 24 hour conditioning period in 3 mg/L $Pb(NO_3)_2$, the sensors were connected to the eDAQ channels in 'biosensor' mode, which applies a constant 10 mV across the sensor and records current changes over time (2000 nA range) at 30 data points per minute. They were then lowered into a 1 L solution of 200 mg/L tris-acetate buffer solution at pH 5.5 (background solution). Prior to spiking the various concentrations of Pb^{2+}, the sensors were left to stabilize in the stirred background solution, then the solution was spiked with Pb^{2+} ions, added from 50 mg/L and 500 mg/L solutions of $Pb(NO_3)_2$ as stock solutions. The current was normalized relative to the baseline current, I_0, calculated by averaging the last 30 measurements (60 s), represented as % response (Eq. 1).

$$\%\, Sensor\ response = \frac{I - I_0}{I_0} \times 100\% \qquad (1)$$

Results and discussion

Optimizing the sensor fabrication for sensitivity

Single-walled carbon nanotubes (SWCNTs) were chosen for the resistive film in the Pb^{2+}-selective chemiresistors since they combine high electrical conductivity with high surface area and chemical stability. For comparison, a batch of sensors including a bare sensor (resistive film: SWCNTs) and three Pb^{2+} sensors (SWCNTs coated with ISM) were fabricated with a previously reported method using copper tape after air-brushing the CNT film and with a circular opening for the ISM. The bare air-brushed CNT films did not show a clear response to Pb^{2+} ions, only a slight decrease in current was observed at higher concentrations whereas the response of the films covered with ISM was clearly notable at 33 µg/L Pb^{2+} (Fig. 8). Although Pb^{2+} detection using ISM-covered CNT-based chemiresistors is a feasible proposition in analogy to previous work with nitrogen species, it does not yet fulfill the requirement of detecting less than 10 µg/L of analyte. A sensor with a resistive film of SWCNTs functionalized with NaOH.15-crown-5 ether solution[34] (f-SWCNTs) was able to detect as little as 10 µg/L Pb^{2+} (Fig. 9) with a maximum average response

of 4.3% at 3.3 mg/L Pb^{2+}. The hydroxide ions are oxidized by the CNTs to form hydrogen peroxide. The reduced nanotubes are negatively charged with n-type behaviour. This negative charge and the presence of oxygen defects on the CNT film facilitate interactions with the cationic crown ether complex, increasing the stability of the percolation network. Hence, the NaOH.15-Crown-5 ether mixture not only n-dopes the CNT film, but also protects the resistive film by forming a highly stable Na^{+}-crown ether complex. As a result, the baseline of the sensor becomes less noisy, so the relative standard deviation (RSD) is reduced, the signal-to-noise (S/N) ratio and also the sensitivity improve (Fig. 2a). Comparing the baseline of the non-functionalized and functionalized resistive films, the S/N ratio increased from 1340 to 1750 and the RSD decreased by 0.19% from 0.76% after functionalization (Fig. 2a). The calculated LoD for the Pb^{2+} sensor with the f-SWCNT film decreased to 10 µg/L.

To lower the LoD even further below 10 µg/L, the sensor geometry was changed to improve contact stability and expose a larger fraction of the resistive film to the ISM. The copper tape contacts were replaced with screen printed carbon contacts, and the aspect ratio of the resistive film was changed using a 3-contact geometry with two narrower channels to enable higher measurement currents at constant film thickness and applied bias. As a result, the S/N ratio of the baseline dramatically increased to 2670 with a lower RSD, 0.38% on average (Fig. 2a). More importantly, the effective surface area using two oval-shape openings (7 mm×18 mm) increased 5-fold over the old fabrication protocol with a circular window (7 mm diameter). The two types of geometries can be compared in Figs. 2b and c. Rectangular windows were not feasible due to membrane detachment in the corners. Since the surface area of the air-brushed CNT film is the same, by this strategy, 55.0% of the CNT film was exposed to the ISM instead of 20.8%. Optimization of fabrication and sensor geometry resulted in detection as low as 3.3 µg/L.

Lead (II) sensor performance

The selected ionophore, lead ionophore IV (tert-Butylcalix[4]arene-tetrakis(N,N-dimethylthioacetamide), is the most sensitive commercially available ionophore for lead (Fig. 3a). A solid-contact ISE made of this ionophore with the same applied membrane composition was reported to operate above 200 µg/L, well above the MAC in drinking water. Even though several improvements to this LoD were reported such as using different conditioning, measuring protocols

and membrane composition, utilizing thin layer technology for applying the ISM, and transduction and amplification of potentiometric signals, a reference electrode was nevertheless required in all cases. Hence, the fabrication of a highly sensitive chemiresistive device for Pb^{2+} detection is a significant achievement, for its simplicity and independence from a reference electrode. First, the performance of the optimized Pb^{2+} sensor was compared to bare and blank sensors. The Pb^{2+} sensor operated selectively and sensitively compared to the bare (f-SWCNT film without the membrane) and the blank (f-SWCNT film coated with a membrane missing the ionophore in its composition). The bare and blank devices did not respond to 10 µg/L Pb^{2+} and responded less than 0.7% to 100 µg/L Pb^{2+} while the ion-selective chemiresistive sensor showed a clear response at 10 µg/L (more than 1%) and 3.0% response to 100 µg/L Pb^{2+} (Fig. 3b).

The clear step-down response of a typical fabricated Pb^{2+} sensor in a concentration range of 3.3 to 3300 µg/L is shown in Fig. 4a. Sensors were immersed in 200 mg/L tris-acetate buffer solution at pH 5.5. The pH 5.5 was chosen as the optimized pH after studying the effect of pH on the sensor response since the sensor at this pH showed slightly higher response than other pHs (Fig. 10). Owing to the properties of the used ionophore, it can be protonated in low pHs and lose its function in complex formation with Pb^{2+}. Also, at pHs higher than 6.5, the formation of $Pb(OH)^{+}$ or/and $Pb(OH)_2$ can decrease the concentration of Pb^{2+} ions in the solution. A representative calibration curve was obtained from averaged data of three cycles of the same sensor (Fig. 11) and error bars were defined as ±standard deviation of three data points at each concentration. (Fig. 4b) The sensor responses were fitted with a Langmuir-style equation (eq. 1). Due to the deviation from the fit at high concentrations, a calibration curve for the lower concentrations is shown in the inset of Fig. 2b. The LoD of the sensor was calculated as 1.75 µg/L. The linearized Langmuir adsorption model, 1/(% - sensor response) vs. $1/[Pb^{2+}]$ is plotted and shown in Fig. 4c.

$$\%-Sensor\ response=\frac{7.53\%\times 0.0048\,ppb^{-1}[Pb^{2+}]}{1+0.0048\,ppb^{-1}[Pb^{2+}]} \qquad (2)$$

The sensors responded more slowly to lower concentrations (Fig. 4d). The average response time for 95% of the response at 3.3 µg/L (the lowest measured detectable concentration) was 8.6 min whereas the average response time at 3300 µg/L (the highest concentration) was 2.3 minutes, with an approximately logarithmic relationship (Fig. 4d). The sensor baseline drift over

three cycles was on average 1.75 pA/s. The RSD as a measure of reproducibility was calculated as 14.5% for an individual sensor. Since each sensor was fabricated by hand, responses from different devices cannot be meaningfully averaged. For device geometry, the best sensor performance in terms of sensitivity and response time was found for a resistance of the deposited CNT film of about 9 kΩ. For optimizing the resistance of the resistive film, three batches of sensors were fabricated (with different range of resistances) the results of which are compared in Table 1. Resistive films with a resistance of about 9 kΩ were more sensitive with lower LoD and faster response to Pb^{2+} ions. The electrical resistance of CNT film is a more accurate representation than "thickness" or "density" of the loosely packed percolation network that forms the film. "Thicker" deposited CNT films (i.e. lower resistances) have slower response times and lower sensitivity while higher resistance (thinner) films demonstrated a little faster response since charge transfer is easier across the film but compared with the optimized resistance (9 kΩ) showed smaller responses with higher LoD. The uniformity of the CNT films in different resistance ranges were investigated by SEM at lower magnifications. The images with 100× magnification show 1×1 mm^2 of the chip, which is 1/100 of the whole surface area of the chip. Overall, the uniformities of the air-brushed CNT films are quite high for all three batches, specifically batch No. 1 and 2 (Fig. 12). Responses of the other sensors in the same range of resistance of batch 1 are shown in Figure 13, which also confirms that each of these sensors is reproducible and reusable.

Table 1 Performance of tested Pb^{2+} sensors in three batches with different resistance ranges of CNT films.

Sensor	Resistance of CNT film (kΩ)	% Sensor response	Lowest detectable concentration (ppb)	Response time at first detectable concentration (s)
Batch No. 1				
Sensor#1	9.2	7.6	3.3	8.6
Sensor#2	9.6	7.5	3.3	8.1
Sensor#3	8.9	7.8	3.3	7.9
Batch No. 2				
Sensor#9	5.5	6.8	10	10.2
Sensor#10	6.1	7.2	10	11.5
Sensor#11	7.8	7.7	3.3	10.9
Batch No. 3				
Sensor#13	12.3	4.3	10	7.5
Sensor#14	12.8	3.8	33	7.2
Sensor#15	13.2	2.9	33	7.8

Due to the properties of ISMs, the Pb^{2+} sensors operated reversibly albeit with slow recovery (Fig. 14). For the recovery test, the sensors were immersed in a background solution (200 mg/L tris/acetate buffer). The sensor averaged a 111.9% recovery after 170 minutes when placed into a lead-free tris-acetate solution at pH 5.5 with an average response of 7.3% (individual cycles: 7.3%, 7.6%, 6.9%) and an average recovery of 8.2% (individual cycles: 7.3%, 8.4%, 8.9%) over three cycles. This slow recovery is likely due to the strong bonding between Pb^{2+} ions and C=S groups in the ionophore. Remarkably, none of the published reports of Pb^{2+} sensors using this ionophore mention a recovery time even though all of them claim that the sensors are reusable with high reproducibility. While the fabricated Pb^{2+} chemiresistive sensor can be reset and reused, this may not be desirable in all application scenarios once lead contamination has been established.

A batch of three sensors were tested in the presence of different interfering ions to determine the feasibility for use in drinking water samples. The tested concentrations of heavy metals and potassium were higher than their common concentrations in drinking water: Hg^{2+} (10 µg/L), Co^{2+} (20 µg/L), Cu^{2+} (20 µg/L), Ni^{2+} (20 µg/L), Cd^{2+} (20 µg/L), Zn^{2+} (100 µg/L), K^{+} (2

mg/L), Pb^{2+} (10 µg/L). Each interferant was added into the background solution in the given order and the sensor response to 10 µg/L Pb^{2+} was tested at the end. No significant interference was observed (Fig. 5) and the data is consistent with reports on potentiometric applications of this ionophore. The sensor response to 10 µg/L Pb^{2+} (-1.15%) in the presence of other heavy metals and 2 mg/L K^+ was also comparable with its response in the absence of these ions (1.16%), confirming that small changes in conductivity do not impact the sensor response to Pb^{2+}.

Real sample test

City of Hamilton tap water (pH=7.45, conductivity 0.29 mS/cm) was collected and filtered through a 0.2 µm Waltman filter paper, pH-adjusted to 5.5 with acetic acid, and stored at 4 °C when not in use. No further sample treatment was done. Several standard solutions of Pb^{2+} ions (3.3, 10, 33, 100 and 330 µg/L) were prepared in tap water. Two sensors were used to measure 10 µg/L Pb^{2+} (to ensure repeatability) and one sensor was tested with 33 µg/L Pb^{2+}. The sensors were immersed in the tap water (0 µg/L Pb^{2+}) overnight and the current was recorded to ensure the sensors were working properly with stable baselines. All sensors were titrated three times to prepare their calibration curves (Figs. 15a-c). Subsequently, the sensors were kept in tap water for 4 hours until a stable baseline was achieved. Two sensors were then immersed in solutions spiked with 10 µg/L Pb^{2+} and one sensor was immersed in 33 µg/L, the solutions were then replaced with blank solutions. The sensor responses were recorded continuously in each case while the jar switching was repeated three times (Figs. 15d-f) and the average response of each sensor reported in Table 2. By comparing the results between the spiked concentrations and found concentrations of each sensor, the average recovery was calculated to be 98.7% with acceptable ranges of error. These Pb^{2+} sensors are therefore promising to be utilized for real world sample analysis. Reagent-free operation can be achieved in combination with water electrolysis to locally acidify the water and avoid formation of $Pb(OH)^+$ and $Pb(OH)_2$.

Table 2 Results of lead sensor to different concentrations of Pb^{2+} in tap water.

Added analyte (µg/L)	Found by sensor (µg/L)	Recovery (%)
0	<3.3	-
10	9.78±0.62	97.98±6.21
10	10.38±0.96	103.86±9.64
33	31.10±0.55	94.24±1.66

Sensing mechanism

A discussion of the sensing mechanism for this sensor needs to consider each step of the fabrication, comparing the responses with and without membrane, as well as of pristine or modified CNT films. Hall measurements (Table 3 and Fig. 6) and Raman spectroscopy (Fig. 16) are also performed to elucidate the behaviour of the resistive film at each step.

Table 3 Hall measurement data of the four-probe device on Si/SiO_2 substrate with sputter coated Au contacts after different fabrication steps, exposure to and removal of Pb^{2+} ions.

Sample	Sheet resistivity (kΩ/sq)	Sheet Hall resistance coef. (m^2/C)	Hall mobility ($cm^2/V.s$)	Sheet concentration (Carrier density) (cm^{-2})
Pristine SWCNT	8.304	2.46	70.7	2.5×10^{14}
f-SWCNT	21.5	-43.2	20.1	-1.4×10^{13}
f-SWCNT coated with ISM	24.04	579	241	1.078×10^{12}
Exposed to 3 ppm of Pb^{2+} for 24 hours	13.76	-14	10.2	-4.461×10^{13}
Washing off Pb^{2+} ions in DI water for 5 hours	9.806	16.9	211	3.69×10^{13}

Exposing a bare device made of pristine SWCNTs to high concentrations of Pb^{2+} (>100 µg/L), a slight decrease in current was observed since the pristine CNT network is slightly p-doped. When Pb^{2+} ions are captured by ionophores in the membrane of an ISM-covered pristine CNT network, the membrane is getting positively charged and acts as a positive electric field gating the p-doped CNT channel, resulting in a drop in current. After addition of the Pb(II) ISM, the same trend was observed but with a higher percentage response at lower concentrations (33 µg/L) compared to the bare and the blank. Hence, the sensor is working based on the same principle with better sensitivity since the membrane preconcentrates the analyte and passes it through to the resistive film (Fig. 8).

The sensor response was expected to invert after modification with the NaOH.15-crown-5 ether mixture due to having a n-type channel being gated by the positive electric field formed by Pb^{2+} ions, resulting in an increase in current. In the devices, however, the same current decrease

was observed as the sensor response. This requires a closer look at the different steps of the fabrication process.

By doing Hall measurement on the device, the sheet resistivity, sheet Hall resistance coefficient, Hall mobility and charge carrier density data were recorded at each step of fabrication (Table 3 and Fig. 6). The Hall coefficient represents the type of the semiconducting (resistive) film, negative values mean it is n-type and positive values show it is p-type. Initially, Hall measurement data confirmed that pristine CNTs were slightly p-doped. After modification with NaOH.15-crown-5 ether mixture the film became slightly n-doped (Table 3 and Figs. 6, 7a), in agreement with previous reports. Data also revealed that the addition of the ISM on top of the resistive film made it highly p-doped. This may be due to an electron-withdrawing effect of the thioamide group in the ionophores on the n-doped CNT film. This interaction between the ionophores and the CNT film is so strong that it can change the dominant charge carriers in the film and make the film p-doped again (Fig. 7b).

According to the Hall measurement data (Table 3 and Fig. 6), the fabricated and ready-to-use sensor initially has a p-doped resistive film. After conditioning the sensor in 3 mg/L Pb^{2+} solution for 24 hours, the Hall coefficient of the device became negative due to the high affinity of the ionophore towards Pb^{2+} ions causing a loss of ionophore-CNT interactions. The complexation is aided by the strong affinity of the thioamide groups for Pb^{2+} and the good fit of the calix[4]arene cavity to the size of Pb^{2+} ions. Because the Pb^{2+} concentration in the conditioning solution was very high, it resulted in reverting the resistive film to n-doped whereas in Pb^{2+} experiments with regular fabricated Pb^{2+} chemiresistive sensors on glass slides in a concentration range of 3.3-3300 µg/L Pb^{2+} the number of holes of the p-type resistive film gets merely reduced upon interaction with the analyte and a decrease in current is observed as the sensor response (Fig. 7c).

The fabricated devices for Hall measurements were left in DI water for 5 hours to remove the Pb^{2+} ions from the device. As it can be seen in Figure 6, “removed Pb^{2+}” step, the Hall coefficient of resistive film returned to positive values as a reverse process. Overall, during the sensor fabrication, measurement and recovery process, the doping type of the CNT film was changed multiple times. Of note, the Hall mobility of the negative charge carriers is always very

low, meaning that the resistance of n-doped films is higher whereas p-doped devices exhibit high Hall mobility values (Table 3 and Fig. 6).

Raman spectroscopy was used to investigate the interactions of the CNT film in more detail, although Raman data could not be obtained from ISM-coated films (Fig. 16). Raman spectra taken from pristine and n-doped CNT films confirm that the 2D band is slightly down-shifted from 2595.5 cm^{-1} to 2592.9 cm^{-1} which is a sign of mild n-doping even though the defect density of the surface has not changed with similar I_D/I_G peak intensity ratios (0.13 to 0.12) (Fig. 16). When the n-doped CNT film was exposed to 3 mg/L Pb^{2+} for 5 hours, it got p-doped and the 2D band up-shifted (from 2592.9 cm^{-1} to 2596.4 cm^{-1}). The CNT percolation network became more disordered as seen by the change in the I_D/I_G ratio from 0.12 to 0.17 (Fig. 16). Indeed, Pb^{2+} ions tend to accept electrons from the surface. Hence, the number of negative charge carriers of the surface decreases and the number of positive charge carriers increases. From the Raman data of the CNT film it can be concluded that n-doping of the CNTs does not change the stability of the CNT film while Pb^{2+} ions interact with the CNT network, p-dope the surface and increase the defect density in agreement with sensor responses and Hall measurement results.

Conclusion

The present disclosure addresses the challenge of improving the LoD of chemiresistive Pb^{2+} sensors to render them suitable for *in situ* continuous monitoring at or below regulatory limits. The CNT structure allows for easy tuning of their electrical properties. Optimizing the network by altering the mobile charge carriers and sensor geometry have a large impact on the sensor performance. A highly sensitive ion-selective chemiresistive sensor for Pb^{2+} detection was built by increasing the effective surface area and stability of the resistive film to increase the S/N ratio and facilitate the interaction with Pb^{2+}. This sensor can detect between 3.3 µg/L and 3300 µg/L Pb^{2+} ions in aqueous solutions with an LoD of 1.75 µg/L which is well below current regulatory limits for lead in drinking water. The detection mechanism is based on the interaction of the ionophores in the ISM with the CNT network in the absence of Pb^{2+} ions. Upon being exposed to Pb^{2+} ions, the ionophores preferentially interact with Pb^{2+} ions, resulting in a decrease in current. This sensor can find applications in the drinking water distribution system, in point-of-use water filters, and in water fountains. It is sensitive, selective, and stable as well as simple to fabricate,

easy to operate, robust, and cost effective. The sensitivity enhancement due to ionophore interactions with the CNT film points the way towards the development of highly sensitive chemiresistors for aqueous ion detection that can surpass the capabilities of potentiometric devices.

The inventors contemplate the possibility of conductive or semiconductive films that that have inherent chemical functionality and directly interact with the ionophore without the use of a ligand. In that context, while carbon nanotubes have been demonstrated to work well, the competitive detection mechanism in which the film competes with the analyte for binding to the ionophore may work for a wider range of substrates, with or without ligand functionalization.

While the above description provides examples of one or more apparatuses or methods, it will be appreciated that other apparatuses or methods may be within the scope of the accompanying claims.

CLAIMS

What is claimed is:

1. A method of making an ion-selective sensor, the method comprising:

providing a conductive or semiconductive film; and

coating the conductive or semiconductive film with an ion-selective membrane comprising at least one ionophore.

2. A method of making an ion-selective sensor, the method comprising:

providing a conductive or semiconductive film;

functionalizing the conductive or semiconductive film with at least one ligand that interacts with the conductive or semiconductive film forming a chemiresistive film; and

coating the conductive or semiconductive film with an ion-selective membrane comprising at least one ionophore.

3. The method of claim 1 or 2, wherein the conductive or semiconductive film comprises at least one single-walled carbon nanotube.

4. The method of claim 3, comprising depositing the at least one single-walled carbon nanotube onto a substrate.

5. The method of claim 4, wherein a resistance of the at least one single-walled carbon nanotube deposited onto the substrate is between 5.5 and 13.2 kΩ.

6. The method of claim 5, wherein the resistance of the at least one single-walled carbon nanotube deposited onto the substrate is about 9 kΩ.

7. The method of any one of claims 2 to 6, wherein the step of functionalizing comprises immersing the at least one single-walled carbon nanotube in a ligand solution.

8. The method of claim 7, comprising immersing the at least one single-walled carbon nanotube in a NaOH.15-crown-5 ether solution.

9. The method of claim 7 or 8, comprising, after the step of functionalizing, curing the sensor at at least 85 °C for at least one hour.

10. The method of any one of claims 1 to 9, wherein the step of coating comprises drop-casting a solution comprising the at least one ionophore.

11. The method of claim 10, comprising, after the step of coating, drying for at least 12 hours.

12. The method claim 10 or 11, comprising conditioning the ion-selective membrane.

13. The method of claim 12, comprising immersing the ion-selective membrane in a Pb(II) salt solution.

14. The method of any one of claims 1 to 13, wherein the at least one ionophore comprises lead ionophore IV.

15. A method of making an ion-selective sensor for analyzing lead ions (Pb^{2+}) in an aqueous solution, the method comprising:

providing at least one single-walled carbon nanotube;

functionalizing the single-walled carbon nanotube with at least one ligand; and

coating the functionalized single-walled carbon nanotube with an ion-selective membrane comprising lead ionophore IV.

16. An ion-selective sensor made according to the method of any one of claims 1 to 15.

17. An ion-selective sensor, comprising:

a conductive or semiconductive film; and

an ion-selective membrane coated on the conductive or semiconductive film and comprising at least one ionophore.

18. The ion-selective sensor of claim 17, wherein the conductive or semiconductive film comprises at least one single-walled carbon nanotube.

19. The ion-selective sensor of claim 17 or 18, wherein the at least one ionophore comprises lead ionophore IV.

20. The ion-selective sensor of any one of claims 16 to 19, wherein the at least one ionophore is configured to competitively bind to the conductive or semiconductive film and analytes in a media.

21. The ion-selective sensor of claim 21, wherein binding sites within the ion-selective membrane are configured to bind with the analytes and modulate interactions between the binding sites and the conductive or semiconductive film.

22. Use of the ion-selective sensor of any one of claims 16 to 21 to analyze analytes in a media.

23. The use of claim 22, wherein the ion-selective sensor monitors lead ions (Pb^{2+}) in an aqueous solution.

24. The use of claim 23, wherein the ion-selective sensor detects between 3.3 µg/L and 3300 µg/L of the Pb^{2+} ions in the aqueous solution.

25. The use of claim 23 or 24, wherein the ion-selective sensor gives a level of detection of about 1.75 µg/L of the Pb^{2+} ions in the aqueous solution.

26. An apparatus or a method comprising any combination of one or more of the features described above and/or claimed above and/or illustrated in the drawings.

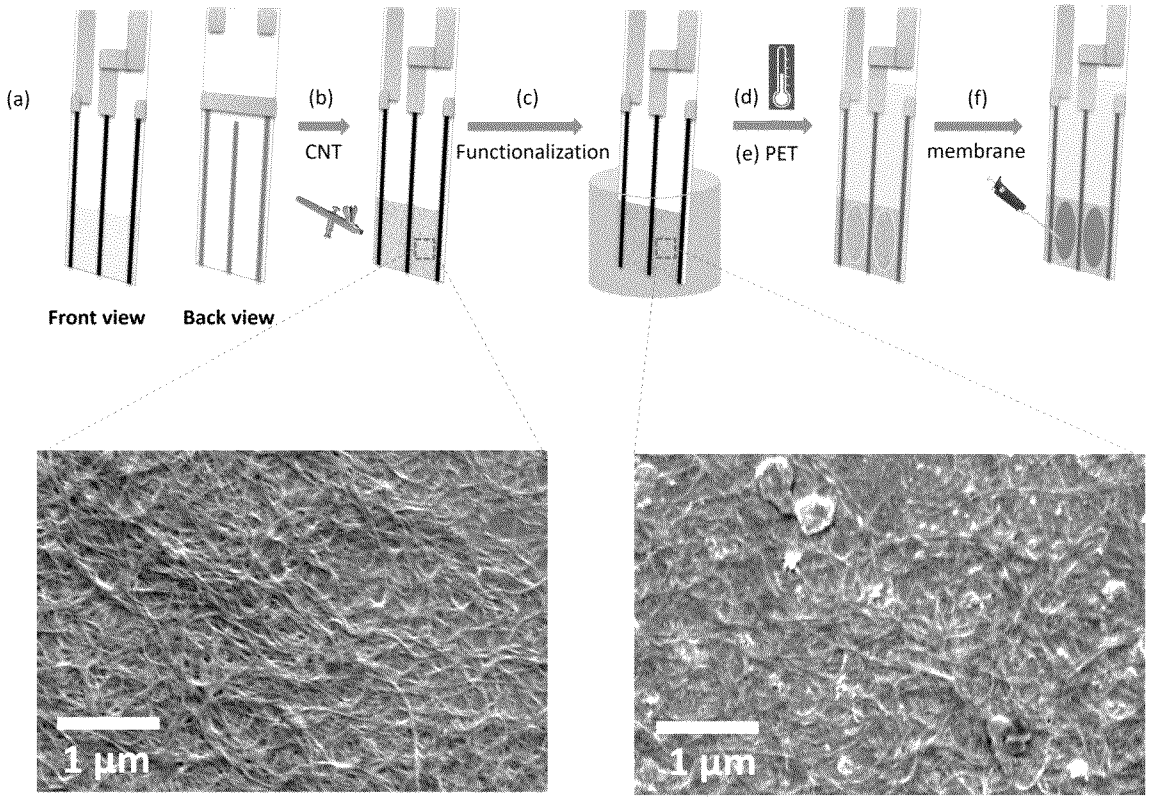
(a)
(b)
CNT
(c)
Functionalization
(d)
(e) PET
(f)
membrane
Front view
Back view
1 µm
1 µm

FIG. 1

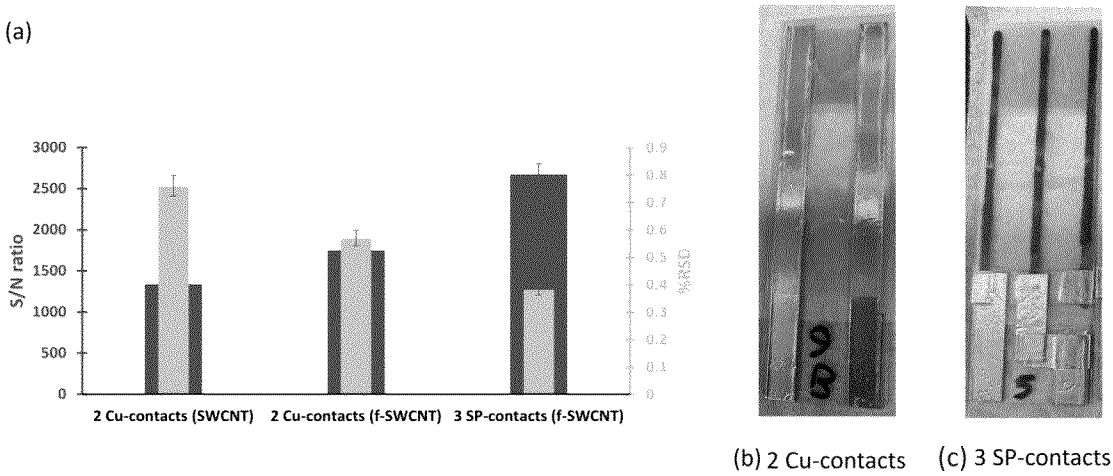
(a)
S/N ratio
%RSD
3000
2500
2000
1500
1000
500
0
0.9
0.8
0.7
0.6
0.5
0.4
0.3
0.2
0.1
0
2 Cu-contacts (SWCNT)
2 Cu-contacts (f-SWCNT)
3 SP-contacts (f-SWCNT)
(b) 2 Cu-contacts
(c) 3 SP-contacts

FIG. 2

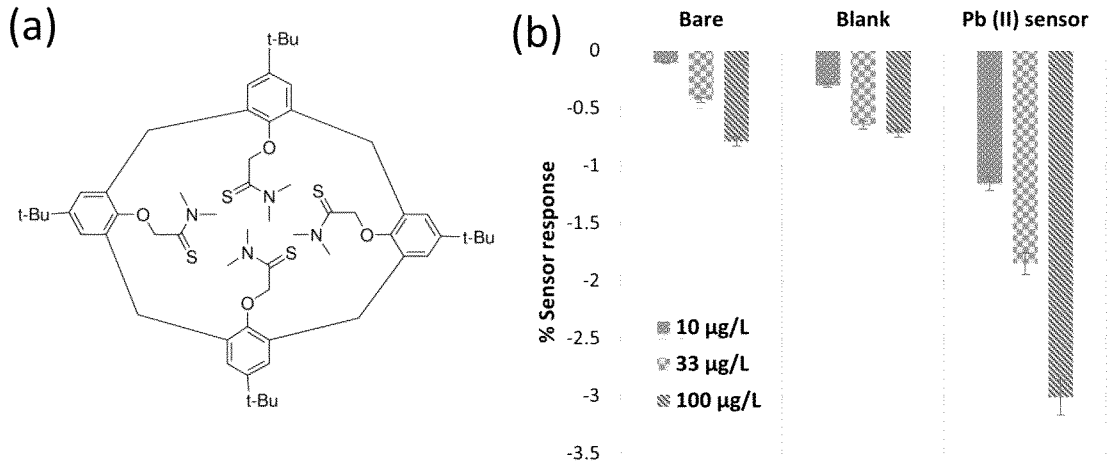
(a)
t-Bu
t-Bu
t-Bu
t-Bu
(b)
Bare
Blank
Pb (II) sensor
% Sensor response
0
-0.5
-1
-1.5
-2
-2.5
-3
-3.5
10 µg/L
33 µg/L
100 µg/L

FIG. 3

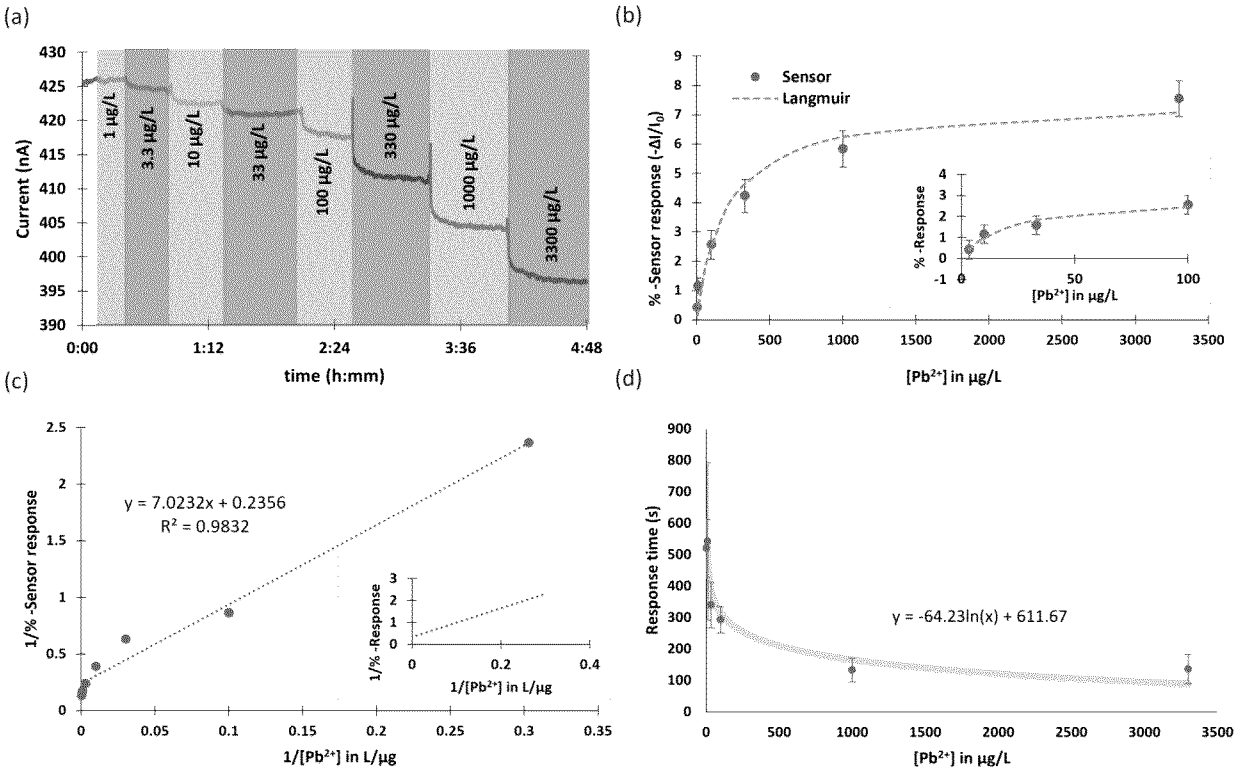
(a)
Current (nA)
time (h:mm)
1 µg/L
3.3 µg/L
10 µg/L
33 µg/L
100 µg/L
330 µg/L
1000 µg/L
3300 µg/L
(b)
Sensor
Langmuir
% -Sensor response (-ΔI/I0)
[Pb2+] in µg/L
% -Response
(c)
y = 7.0232x + 0.2356
R² = 0.9832
1/% -Sensor response
1/[Pb2+] in L/µg
1/% -Response
(d)
Response time (s)
y = -64.23ln(x) + 611.67
[Pb2+] in µg/L

FIG. 4

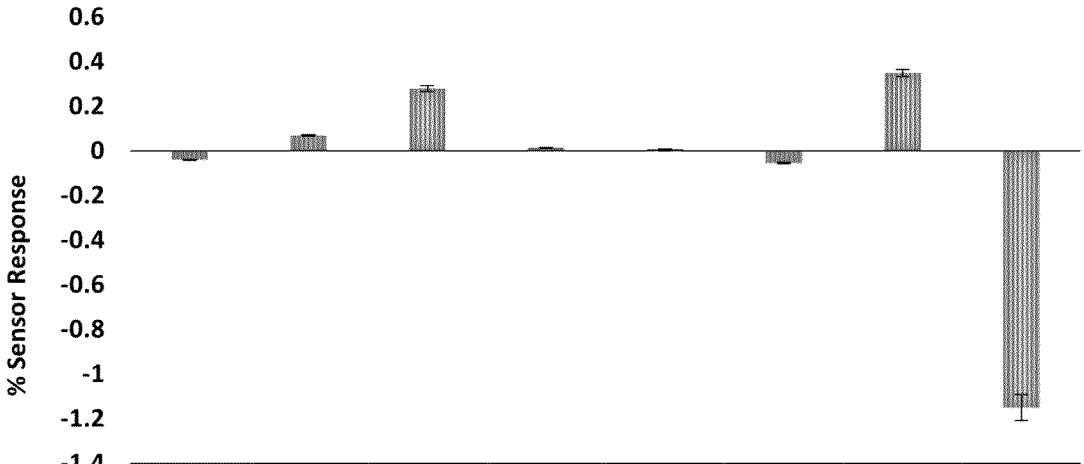

	10 µg/L Hg (II)	20 µg/L Co (II)	20 µg/L Cu (II)	20 µg/L Ni (II)	20 µg/L Cd (II)	100 µg/L Zn (II)	2 mg/L K+	10 µg/L Pb (II)
sensor	-0.04	0.07	0.28	0.015	0.01	-0.054	0.35	-1.15

FIG. 5

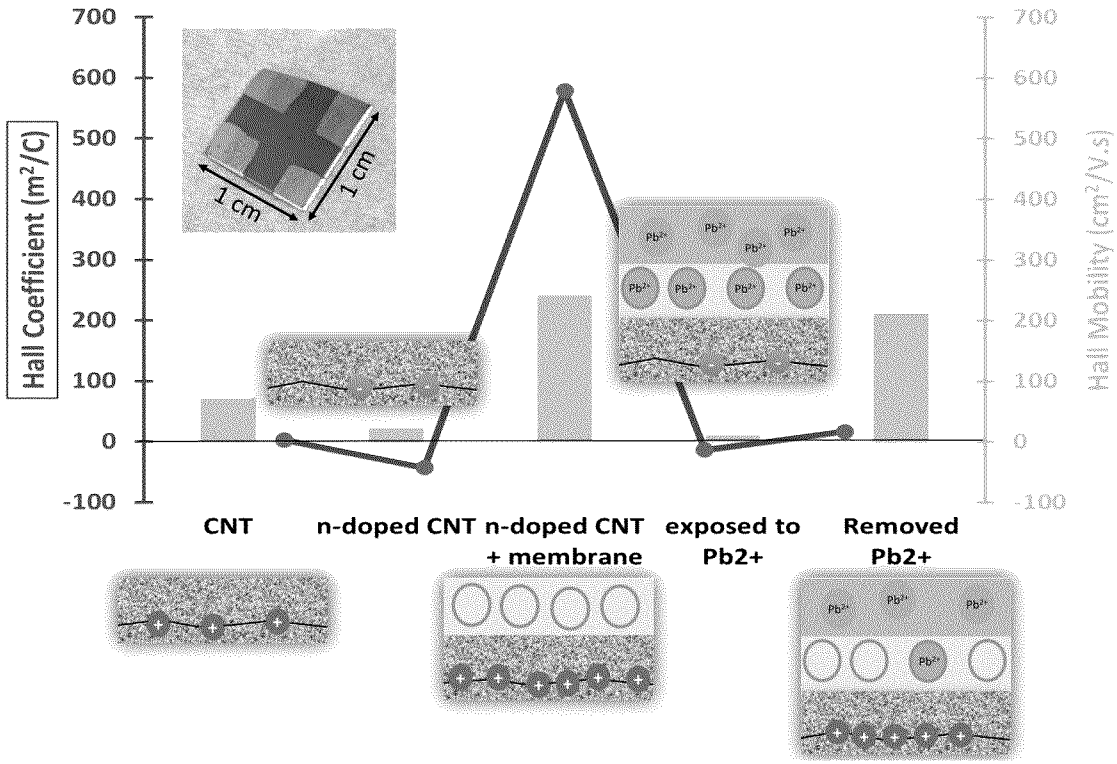
Hall Coefficient (m²/C)
Hall Mobility (cm²/V.s)
700
600
500
400
300
200
100
0
-100
1 cm
1 cm
Pb2+
CNT
n-doped CNT
n-doped CNT + membrane
exposed to Pb2+
Removed Pb2+

FIG. 6

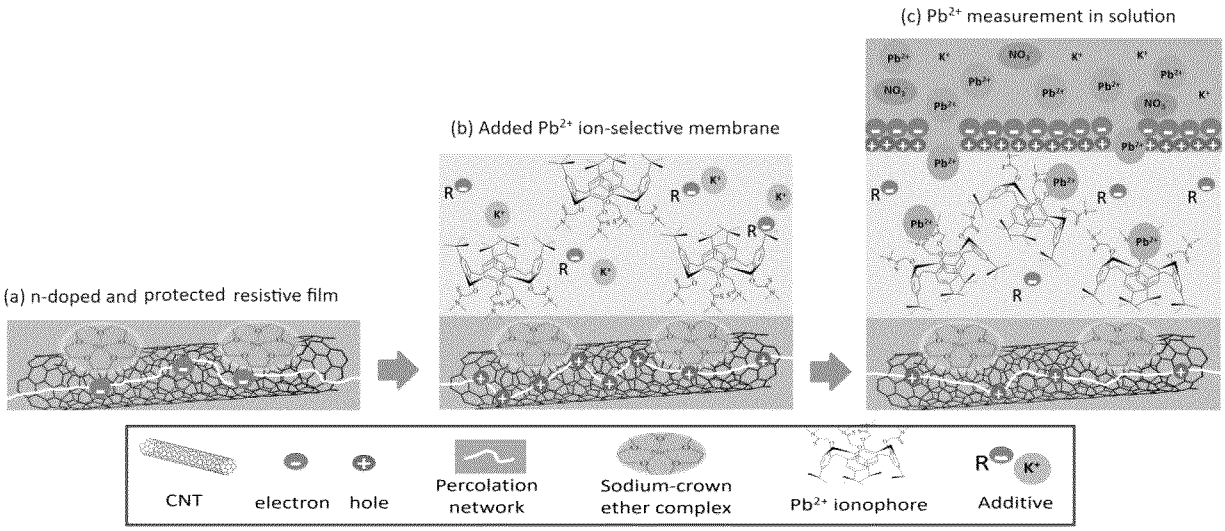
(a) n-doped and protected resistive film
(b) Added Pb2+ ion-selective membrane
(c) Pb2+ measurement in solution
CNT
electron
hole
Percolation network
Sodium-crown ether complex
Pb2+ ionophore
Additive

FIG. 7

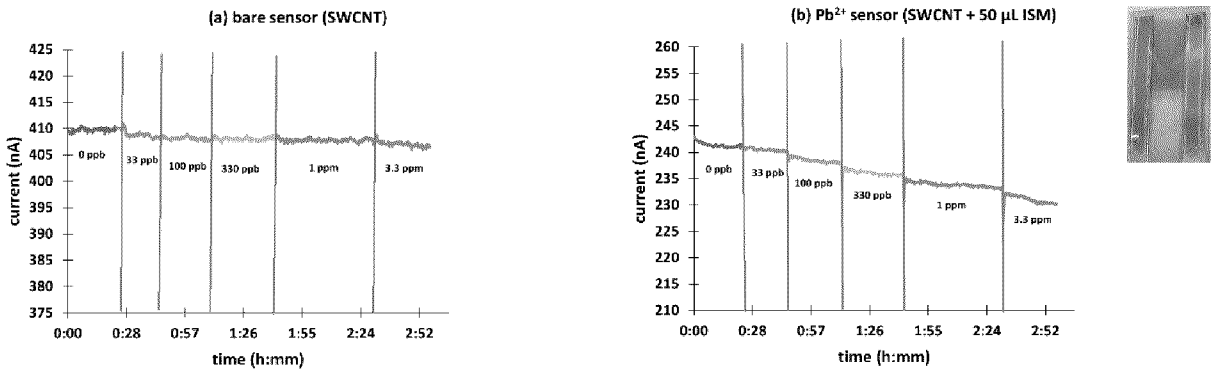
(a) bare sensor (SWCNT)
current (nA)
time (h:mm)
0 ppb
33 ppb
100 ppb
330 ppb
1 ppm
3.3 ppm
(b) Pb2+ sensor (SWCNT + 50 µL ISM)
current (nA)
time (h:mm)
0 ppb
33 ppb
100 ppb
330 ppb
1 ppm
3.3 ppm

FIG. 8

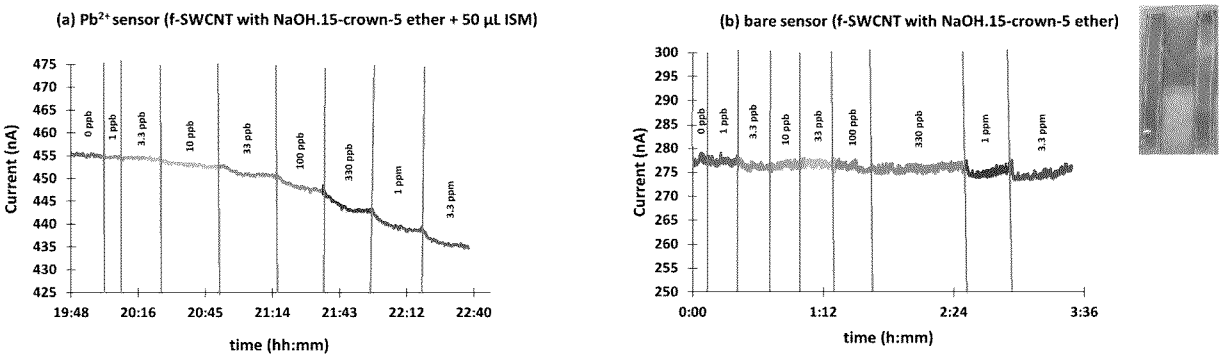
(a) Pb2+ sensor (f-SWCNT with NaOH.15-crown-5 ether + 50 µL ISM)
Current (nA)
time (hh:mm)
0 ppb
1 ppb
3.3 ppb
10 ppb
33 ppb
100 ppb
330 ppb
1 ppm
3.3 ppm
(b) bare sensor (f-SWCNT with NaOH.15-crown-5 ether)
Current (nA)
time (h:mm)
0 ppb
1 ppb
3.3 ppb
10 ppb
33 ppb
100 ppb
330 ppb
1 ppm
3.3 ppm

FIG. 9

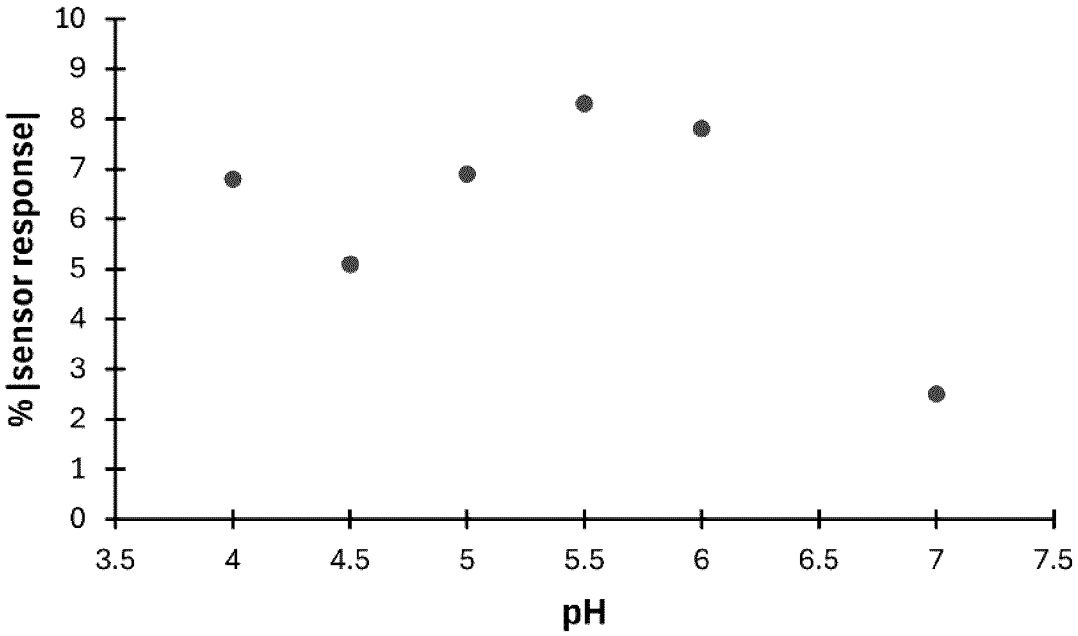

FIG. 10

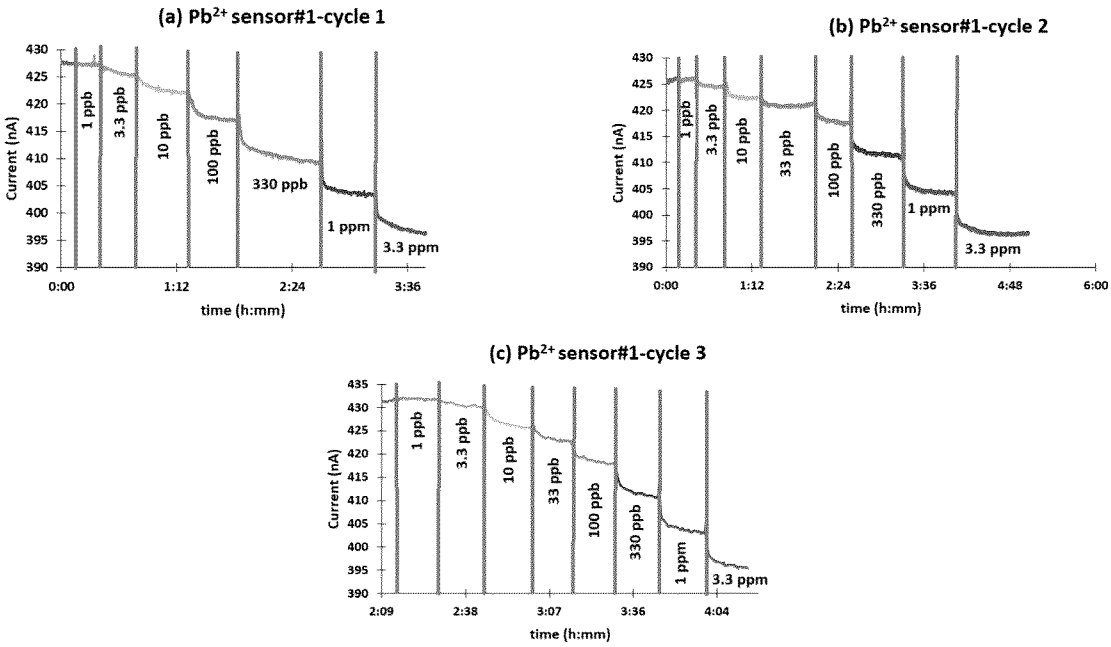
(a) Pb2+ sensor#1-cycle 1
Current (nA)
time (h:mm)
1 ppb
3.3 ppb
10 ppb
100 ppb
330 ppb
1 ppm
3.3 ppm
(b) Pb2+ sensor#1-cycle 2
Current (nA)
time (h:mm)
1 ppb
3.3 ppb
10 ppb
33 ppb
100 ppb
330 ppb
1 ppm
3.3 ppm
(c) Pb2+ sensor#1-cycle 3
Current (nA)
time (h:mm)
1 ppb
3.3 ppb
10 ppb
33 ppb
100 ppb
330 ppb
1 ppm
3.3 ppm

FIG. 11

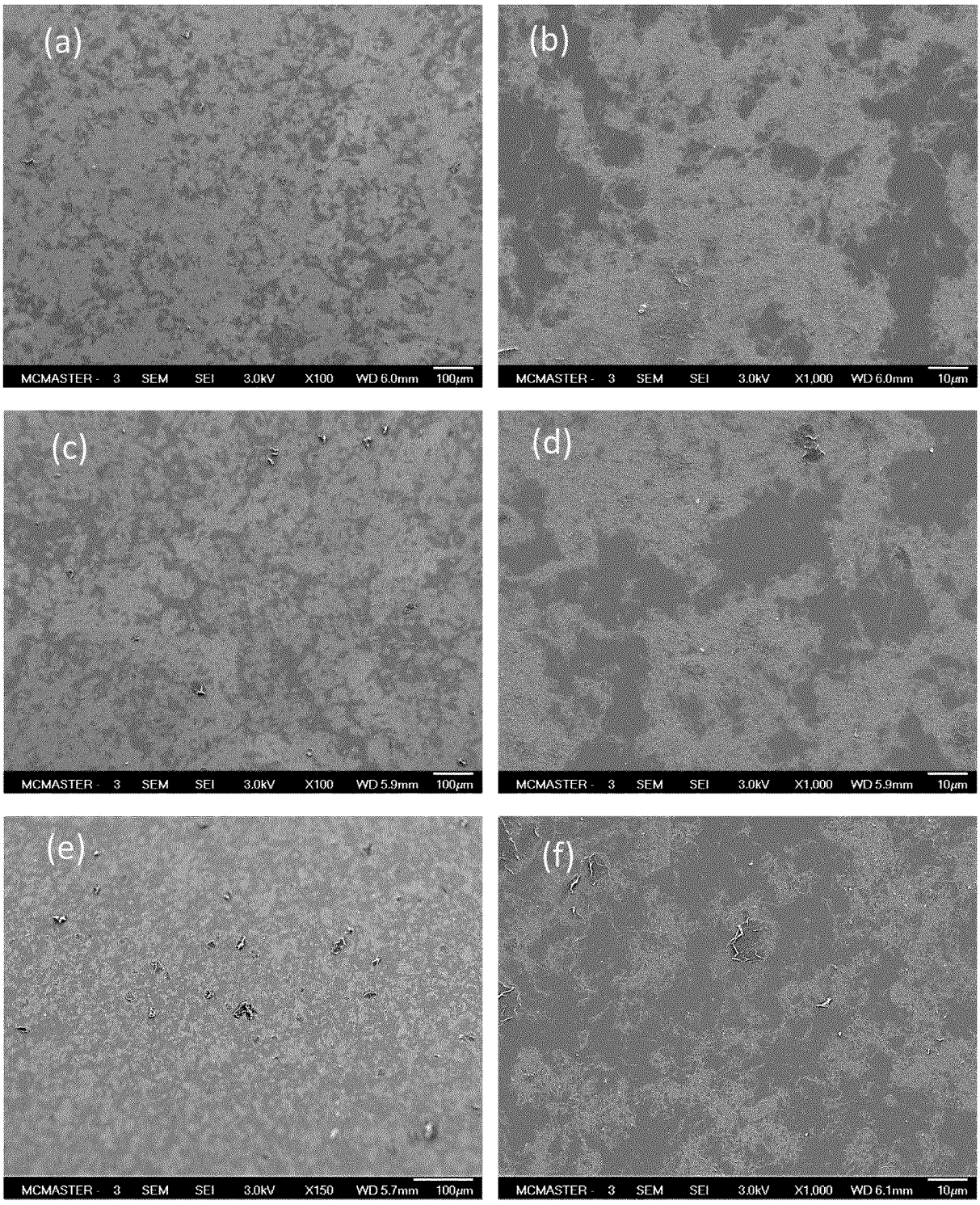
(a)
MCMASTER - 3 SEM SEI 3.0kV X100 WD 6.0mm 100μm
(b)
MCMASTER - 3 SEM SEI 3.0kV X1,000 WD 6.0mm 10μm
(c)
MCMASTER - 3 SEM SEI 3.0kV X100 WD 5.9mm 100μm
(d)
MCMASTER - 3 SEM SEI 3.0kV X1,000 WD 5.9mm 10μm
(e)
MCMASTER - 3 SEM SEI 3.0kV X150 WD 5.7mm 100μm
(f)
MCMASTER - 3 SEM SEI 3.0kV X1,000 WD 6.1mm 10μm

FIG. 12

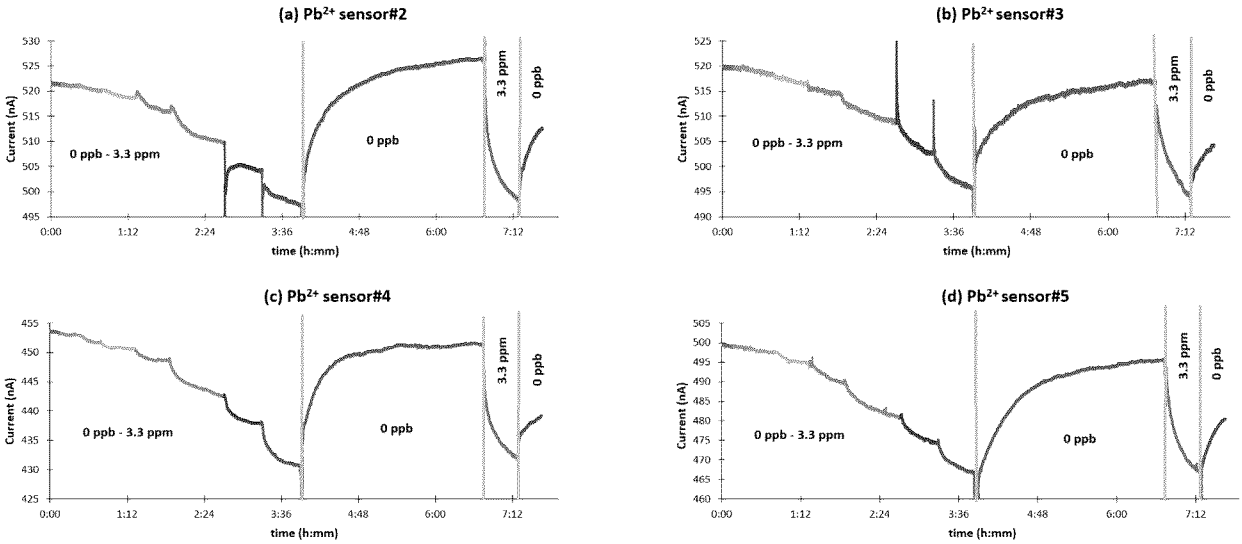
(a) Pb2+ sensor#2
(b) Pb2+ sensor#3
(c) Pb2+ sensor#4
(d) Pb2+ sensor#5
Current (nA)
time (h:mm)
0 ppb - 3.3 ppm
0 ppb
3.3 ppm
0 ppb

FIG. 13

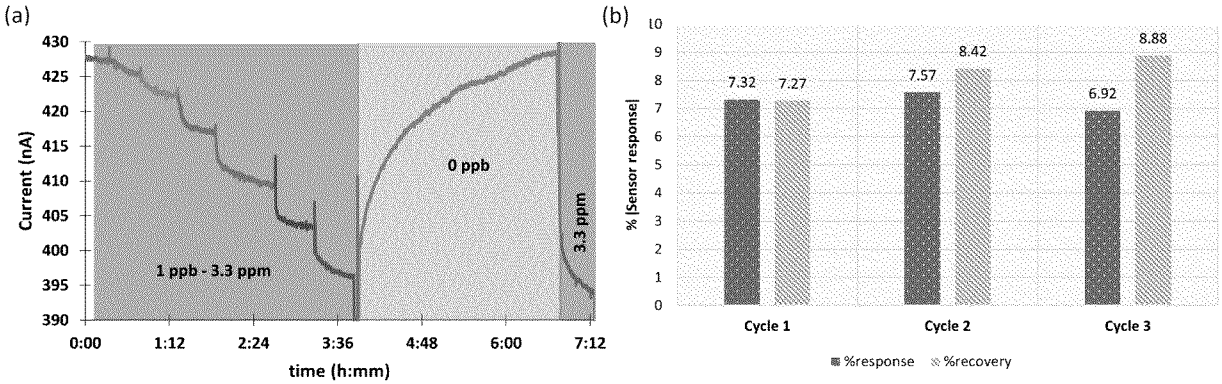
(a)
Current (nA)
time (h:mm)
1 ppb - 3.3 ppm
0 ppb
3.3 ppm
(b)
% |Sensor response|
7.32
7.27
7.57
8.42
6.92
8.88
Cycle 1
Cycle 2
Cycle 3
%response
%recovery

FIG. 14

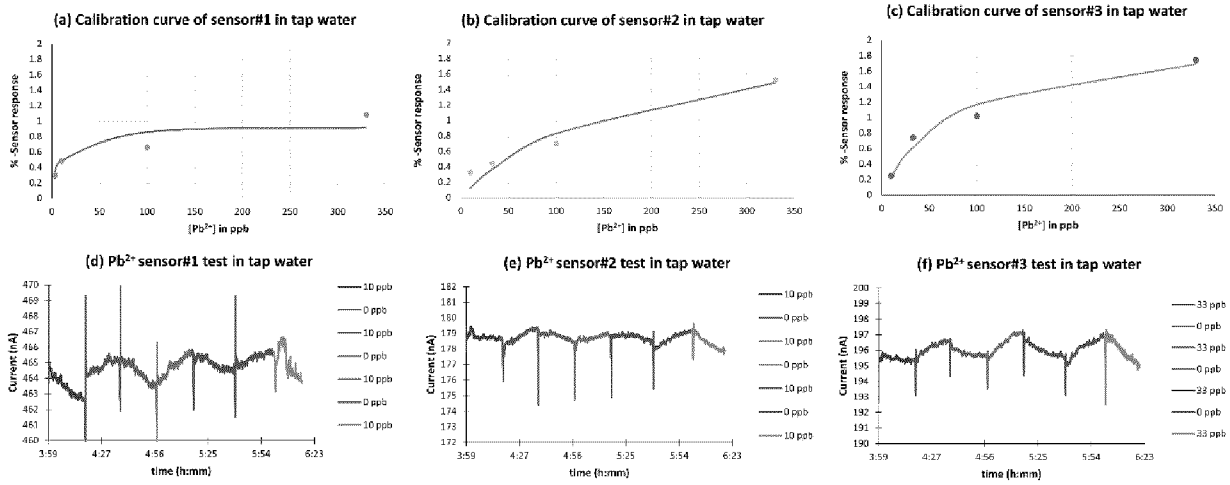
(a) Calibration curve of sensor#1 in tap water
% -Sensor response
[Pb2+] in ppb
(b) Calibration curve of sensor#2 in tap water
% -Sensor response
[Pb2+] in ppb
(c) Calibration curve of sensor#3 in tap water
% -Sensor response
[Pb2+] in ppb
(d) Pb2+ sensor#1 test in tap water
Current (nA)
time (h:mm)
10 ppb
0 ppb
10 ppb
0 ppb
10 ppb
0 ppb
10 ppb
(e) Pb2+ sensor#2 test in tap water
Current (nA)
time (h:mm)
10 ppb
0 ppb
10 ppb
0 ppb
10 ppb
0 ppb
10 ppb
(f) Pb2+ sensor#3 test in tap water
Current (nA)
time (h:mm)
33 ppb
0 ppb
33 ppb
0 ppb
33 ppb
0 ppb
33 ppb

FIG. 15

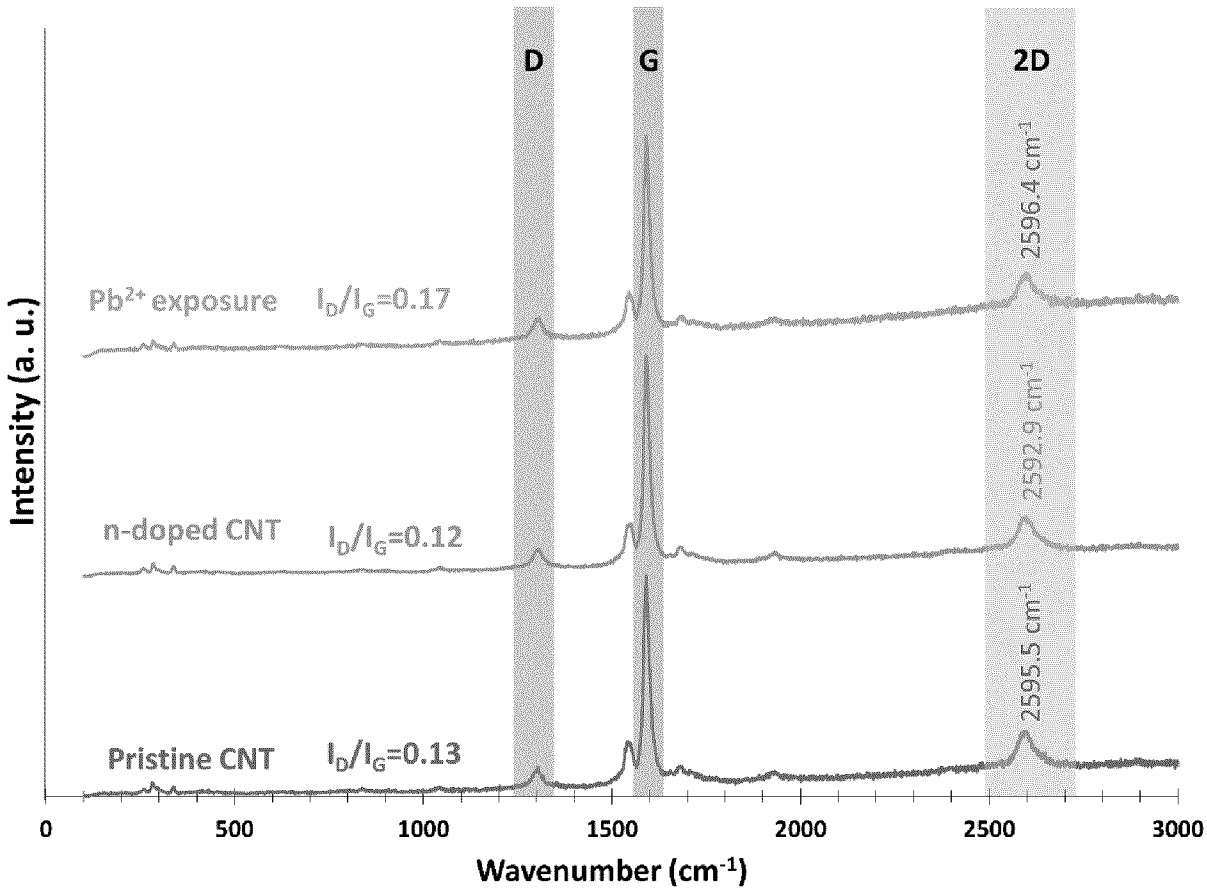
D
G
2D
2596.4 cm-1
2592.9 cm-1
2595.5 cm-1
Pb2+ exposure ID/IG=0.17
n-doped CNT ID/IG=0.12
Pristine CNT ID/IG=0.13
Intensity (a. u.)
0
500
1000
1500
2000
2500
3000
Wavenumber (cm-1)

FIG. 16

INTERNATIONAL SEARCH REPORT

International application No.
PCT/CA2024/051696

A. CLASSIFICATION OF SUBJECT MATTER

IPC: ***G01N 27/12*** (2006.01)

CPC: G01N 27/12 (2017.08)

According to International Patent Classification (IPC) or to both national classification and IPC

B. FIELDS SEARCHED

Minimum documentation searched (classification system followed by classification symbols)
IPC: G01N 27, C01B 32/174.
CPC: G01N 27/04, C01B 32/174, G01N 27/12.

Documentation searched other than minimum documentation to the extent that such documents are included in the fields searched
(n.a.)

Electronic database(s) consulted during the international search (name of database(s) and, where practicable, search terms used)

(See 1st page of extra sheet.)

C. DOCUMENTS CONSIDERED TO BE RELEVANT

Category*	Citation of document, with indication, where appropriate, of the relevant passages	Relevant to claim No.
X, P	DARESTANI-FARAHANI, Maryam, MONTEALEGRE, Isabella Mendoza, GILAVAN, Mehraneh Tavakkoli, et al. A highly sensitive ion-selective chemiresistive sensor for online monitoring of lead ions in water. Analyst, 2024, vol. 149, no 10, p. 2915-2924.	
X	DARESTANI-FARAHANI, Maryam, MA, Fanqing, PATEL, Vinay, et al. An ion-selective chemiresistive platform as demonstrated for the detection of nitrogen species in water. Analyst, 10.10.2023, vol. 148, no 22, p. 5731-5744.	1, 3 to 6, 10 to 12, 16 to 18, 22
X	YU, Shunyang, LI, Fuhai, YIN, Tanji, et al. A solid-contact Pb2+-selective electrode using poly (2-methoxy-5-(2′-ethylhexyloxy)-p-phenylene vinylene) as ion-to-electron transducer. Analytica chimica acta, 2011, vol. 702, no 2, p. 195-198.	1, 10, 12 to 14, 16, 17, 19, 22 to 25

☒ Further documents are listed in the continuation of Box C. ☐ See patent family annex.

*	Special categories of cited documents:	"T"	later document published after the international filing date or priority date and not in conflict with the application but cited to understand the principle or theory underlying the invention
"A"	document defining the general state of the art which is not considered to be of particular relevance	"X"	document of particular relevance; the claimed invention cannot be considered novel or cannot be considered to involve an inventive step when the document is taken alone
"D"	document cited by the applicant in the international application	"Y"	document of particular relevance; the claimed invention cannot be considered to involve an inventive step when the document is combined with one or more other such documents, such combination being obvious to a person skilled in the art
"E"	earlier application or patent but published on or after the international filing date	"&"	document member of the same patent family
"L"	document which may throw doubts on priority claim(s) or which is cited to establish the publication date of another citation or other special reason (as specified)		
"O"	document referring to an oral disclosure, use, exhibition or other means		
"P"	document published prior to the international filing date but later than the priority date claimed		

Date of the actual completion of the international search 06 January 2025 (06.01.2025)	Date of mailing of the international search report 07 January 2025 (07-01-2025)
Name and mailing address of the ISA/CA Canadian Intellectual Property Office Place du Portage I, C114 - 1st Floor, Box PCT 50 Victoria Street Gatineau, Quebec K1A 0C9 Facsimile No.: 819-953-2476	Authorized officer Christian Barrette (819) 639-8421

C (Continuation). DOCUMENTS CONSIDERED TO BE RELEVANT

Category*	Citation of document, with indication, where appropriate, of the relevant passages	Relevant to claim No.
A	DALMIEDA, Johnson, ZUBIARRAIN-LASERNA, Ana, GANEPOLA, Devanjith, et al. Chemiresistive detection of silver ions in aqueous media. Sensors and Actuators B: Chemical, 2021, vol. 328, p. 129023.	
A	DEB, Madhurima, SAXENA, Sumit, BANDYOPADHYAYA, Rajdip, et al. β-Cyclodextrin functionalized rGO films for lead sensing. Materials Science and Engineering: B, 2021, vol. 272, p. 115323.	
A	DALMIEDA, Johnson, ZUBIARRAIN-LASERNA, Ana, SAHA, Dipankar, et al. Impact of surface adsorption on metal–ligand binding of phenanthrolines. The Journal of Physical Chemistry C, 2021, vol. 125, no 38, p. 21112-21123.	
A	MENG, Zheng, STOLZ, Robert M., MENDECKI, Lukasz, et al. Electrically-transduced chemical sensors based on two-dimensional nanomaterials. Chemical reviews, 2019, vol. 119, no 1, p. 478-598.	

INTERNATIONAL SEARCH REPORT

International application No.
PCT/CA2024/051696

Box No. II Observations where certain claims were found unsearchable (Continuation of item 2 of the first sheet)

This international search report has not been established in respect of certain claims under Article 17(2)(a) for the following reasons:

1. ☐ Claim Nos.:
because they relate to subject matter not required to be searched by this Authority, namely:

2. ☒ Claim Nos.: 26
because they relate to parts of the international application that do not comply with the prescribed requirements to such an extent that no meaningful international search can be carried out, specifically:

Claim 26 does not comply with Rule 6.2(a) pursuant to which "[c]laims shall not, except where absolutely necessary, rely, in respect of the technical features of the invention, on references to the description or drawings." Claim 26 relies indefinitely on references both to the description and the drawings.

3. ☐ Claim Nos.:
because they are dependent claims and are not drafted in accordance with the second and third sentences of Rule 6.4(a).

Box No. III Observations where unity of invention is lacking (Continuation of item 3 of first sheet)

This International Searching Authority found multiple inventions in this international application, as follows:

1. ☐ As all required additional search fees were timely paid by the applicant, this international search report covers all searchable claims.

2. ☐ As all searchable claims could be searched without effort justifying additional fees, this Authority did not invite payment of additional fees.

3. ☐ As only some of the required additional search fees were timely paid by the applicant, this international search report covers only those claims for which fees were paid, specifically claim Nos.:

4. ☐ No required additional search fees were timely paid by the applicant. Consequently, this international search report is restricted to the invention first mentioned in the claims; it is covered by claim Nos.:

Remark on Protest

☐ The additional search fees were accompanied by the applicant's protest and, where applicable, the payment of a protest fee.

☐ The additional search fees were accompanied by the applicant's protest but the applicable protest fee was not paid within the time limit specified in the invitation.

☐ No protest accompanied the payment of additional search fees.

(Continuation of second sheet, section B, "Electronic database(s) consulted during the international search".)

Below is the journal of exact search steps performed, in chronological order.

Basis	Engine	Database or tool	Search string, cited document or citing document	Hits, or number of citations	Reviewed
Backward citation	(n.a.)	(n.a.)	Examined description	10	1-10[1]
Keyword	STNext	INDEX ALL	S chemiresistor [L1] D RANK [Best database identified: Caplus]	(n.a.)	(n.a.)
		Caplus	S chemiresist? AND ("Ionophores"+UF,OLD/CT OR ionophor?) [L2]	2	1-2[2]
Backward citation	(n.a.)	(n.a.)	[2]DARESTANI-FARAHANI, Maryam, MONTEALEGRE, Isabella Mendoza, GILAVAN, Mehraneh Tavakkoli, et al. A highly sensitive ion-selective chemiresistive sensor for online monitoring of lead ions in water. Analyst, 2024, vol. 149, no 10, p. 2915-2924.	58	1, 7-9, 17, 28-30, 40, 44, 46-49[3]
			[3]KRUSE, Peter. Review on water quality sensors. Journal of Physics D: Applied Physics, 2018, vol. 51, no 20, p. 203002.	271	135
Author/ inventor	STNext	Caplus	S ("KRUSE P"/AU OR "KRUSE P D"/AU OR "KRUSE P E"/AU OR "KRUSE P F JR"/AU OR "KRUSE P J"/AU OR "KRUSE P W"/AU) OR ("KRUSE PETER"/AU OR "KRUSE PETER D"/AU OR "KRUSE PETER W"/AU) [L1]	141	(none)
			S ("DARESTANI FARAHANI M"/AU OR "DARESTANI FARAHANI MARYAM"/AU) OR "DARESTANI MARIAM T"/AU [L2]	11	(none)
			S ("SELVAGANAPATHY P R"/AU OR "SELVAGANAPATHY P RAVI"/AU OR "SELVAGANAPATHY PONNAMBALAM"/AU OR "SELVAGANAPATHY PONNAMBALAM R"/AU OR "SELVAGANAPATH Y PONNAMBALAM RAVI"/AU OR "SELVAGANAPATHY R"/AU OR "SELVAGANAPATHY RAVI"/AU) [L3]	191	(none)
			S L1-L3 [L4]	311	(none)
Owner	STNext	Caplus	S McMaster/CS [L5]	35 717	(none)
Combined	STNext	Caplus	S L4-L5 AND chemiresist?/BI,CLM [L6]	26	1-26
Classification	STNext	Caplus	S (G01N0027? OR C01B0032-174)/IPC [L1]	179 260	(none)
			S (G01N0027/04? OR C01B0032-174)/CPC [L2]	7688	(none)
			S L1-L2 [L3]	180 244	(none)
			S L3 AND "Ionophores" [L4]	341	(none)
			S L4 AND "Ion-selective membranes" [L5]	65	(none)
			S L3 AND chemiresist?/BI,CLM [L6]	211	(none)
			S L6 AND "Ion-selective membranes" [L7]	1	1-1

(Continued on 2nd page of extra sheet.)

(Continuation of second sheet, 1st page.)

Basis	Engine	Database or tool	Search string, cited document or citing document	Hits, or number of citations	Reviewed
Author/ inventor	Google Scholar	2023	chemiresistors author:kruse OR author:darestani OR author:SELVAGANAPATHY	4	1-4
Forward citation	Google Scholar	"Cited by"	ARIDA, H. A., AL-HADDAD, A., SCHÖNING, M. J. New solid-state organic membrane based leadselective micro-electrode. In: Computational Methods and Experimental Measurements XV. WIT Transactions on Modelling and Simulation, 2011, vol. 51, p. 547-557.	6	1-6
Keyword	Google Scholar	Excluding patents	chemiresistors "ion-selective membrane"	111	(none)
			chemiresistors "ion-selective membrane" ionophore	75	1-75[4]
Backward citation	(n.a.)	(n.a.)	[4]HEIN, Robert et BEER, Paul D. Halogen bonding and chalcogen bonding mediated sensing. Chemical Science, 2022, vol. 13, no 24, p. 7098-7125.	186	168-170, 173
			[4]MENG, Zheng, STOLZ, Robert M., MENDECKI, Lukasz, et al. Electrically-transduced chemical sensors based on two-dimensional nanomaterials. Chemical reviews, 2019, vol. 119, no 1, p. 478-598.	1 129	533
Keyword	Google Patents	(n.a.)	chemiresistors "ion-selective membrane" ionophore	1	1-1
Classification	STNext	Caplus	S G01N0027/12?/CPC [L1]	9696	(none)
			S L1 AND chemiresist?/BI,CLM [L2]	153	(none)
			S L2 AND "Ion-selective membranes" [L3]	0	(n.a.)
			S L2 AND membran? [L4]	5	1-5